Available at www.scientevents.com/proscience/

ScientEvents

ProScience 10 (2026) 47-52

ProScience

Conference Proceedings

International Conference on Microwave and High Frequency Applications - AMPERE 2025

Microwave-Assisted Combustion Synthesis of intermetallic composites from recycled powders

Magdalena Lassinantti Gualtieri*, Elena Colombini, Paolo Veronesi

Department of Engineering "Enzo Ferrari", University of Modena and Reggio Emilia, Via P. Vivarelli 10/1, 41125 Modena, Italy

**Magdalena.gualtieri@unimore.it*

Abstract

This work deals with the synthesis of *in situ* intermetallic matrix composites using spent powders from additive manufacturing as raw materials and microwave energy for ignition of combustion synthesis reactions between aluminum and 3d transition metals (nickel and titanium). The powders derived from selective laser melting manufacturing of components for automotive in nickel-based super alloys (Inconel 625) and lightweight aluminum (AlSi10Mg) and titanium (Ti6Al4V) alloys. The powders were combined in the pseudo-binary systems NiAl (30-70 at.% aluminum) and TiAl (50-70 at.% aluminum). Minor additional metals (Cr, Mo, Nb and Fe, V, Mg) and metalloids (Si) were introduced from the recycled powders themselves giving the possibility to obtain interesting multi-phase microstructures and microalloying of the main nickel and titanium aluminides. Microstructural investigations were performed by X-ray diffraction (XRD) and scanning electron microscopy imaging coupled with energy-dispersive X-ray spectroscopy (SEM-EDS). It is shown that the NiAl-based system mainly results in near to equiaxed grains of B2 NiAl surrounded by a complex intergranular region with a fine microstructure. Main phases in this region are microalloyed chromium silicides, Laves C14 $NbSi_2$ and tetragonal σ-phase (in Ni-rich samples). In compositions with highest amount of Al, more complex nickel aluminides are formed (Al_3Ni_2, Al_3Ni). The TiAl-system contains the titanium aluminides predicted from phase diagrams in addition to Si_3Ti_5. The use of recycled alloy powders and energetically efficient ignition by microwaves has high potential for obtaining sustainable intermetallic composites without the need for additional alloying.

Keywords: Intermetallic composites; combustion synthesis; microwave ignition; powder recycling

ISSN: 2283-5954
Selection and peer-review under responsibility of AMPERE 2025 Scientific Committee
DOI:10.14644/microwave2025.009

1. Introduction

Aluminides of Ni and Ti has potential for lightweight structural materials operating at high temperature (Yamaguchi et al., 2000; Darolia, 1991). The Al-Ni binary phase diagram includes five stable phase at ambient temperature (Al_3Ni with $D0_{11}$ structure; Al_3Ni_2 with $D5_{13}$ structure, NiAl with B2 structure, Al_3Ni_5 and $AlNi_3$ with $L1_2$ structure) in addition to solid solutions of Al and Ni with fcc structure (Shao et al., 2023). The most important nickel aluminides for structural applications are $AlNi_3$ (Deevi & Sikk 1996) and NiAl (Darolia, 1991) as they maintain long-range order up to the melting temperature (Zharov, 2023). An interesting aspect of NiAl is that it covers a wide field of the Al-Ni phase diagram, extending from 45 to 60 at. % Ni (Shao et al. 2023). The B2 NiAl structure can be non-stoichimoetric containing vacancies or anti-site substitutions. Hence, deviations from stoichiometry and alloying give the possibility to tailor phase properties. In Ni-rich B2 structures, the central Al atom is replaced by Ni which leads to smaller lattice constant and higher density (Ni being smaller and heavier than Al) (Xiao & Baker, 1994). On the contrary, a higher Al:Ni ratio leads to both vacancies and anti-site substitution on the Ni-sites (Xiao & Baker, 1994). The density decreases (Al lighter than Ni) as does the lattice constant (presence of vacancies). Hence, the stoichiometric NiAl shows a maximum in density and lattice constant, a trend that is translated to similar ones regarding both physical and mechanical properties (Noebe et al. 1993). The type and degree of B2 structural defect can thus be used to tune desired properties.

The Al-Ti binary phase diagram shows six stable phases at ambient temperature: Ti with A3 structure; Ti_3Al with $D0_{19}$ structure; TiAl with $L1_0$ structure; $TiAl_2$ (HfGa structure type); $TiAl_3$ ($D0_{22}$) and Al with A1 structure (Schuster & Palm, 2006). Common Titanium aluminate alloys are two-phased systems containing both TiAl and Ti_3Al (Genc & Unal, 2022). Much work has also been dedicated to Al_3Ti alloys, mainly motivated by the very low density and high corrosion resistance (Diao et al., 2024).

Although Ni and Ti aluminides offer major advantages over conventional high-temperature structure materials (low-density materials with higher melting temperature and thermal conductivity) broader applications are limited due to low ductility at room temperature and limited strength at high temperature. Common ways for improvements are micro- and macroalloying leading to atomic substitutions in the aluminide phase (Cotton et al, 1993), finer gran size and changed morphology (Paul et al., 2024) and multi-phase systems produced *in situ* (intermetallic matrix composites, IMC) (Awotunde et al. 2019). For example, NiAl-based eutectic alloys such as the NiAl-Cr and NiAl-Cr(Mo) have been extensively investigated (Wang et al., 2022). A highly studied *in situ* IMC in the TiAl system is Ti_5Si_3 reinforced TiAl (Novák et al., 2009). Recently, much work has also been dedicated to the Al_3Ti phase where the addition of multiple additional elements transforms the brittle DO_{22} phase to ductile $L1_2$ phase and contemporary introduced hard secondary phases to compensate for the strength loss accompanied by the phase change (Diao et al., 2024).

A common and simple manufacturing method of bulk Ni and Ti aluminides and *in situ* intermetallic matrix composites is through combustion synthesis reactions between elemental powders ignited by some external energy source (Rosa et al., 2013). The transformation from pure elements to alloys may occur either through a combustion wave starting from one point of the sample (i.e. self-propagating high temperature synthesis (SHS)) or by thermal explosion (TE) where controlled heating of the powder mixture leads to simultaneous ignition of the combustion reactions in each point of the sample volume. Combustion synthesis offers several advantages, including energy efficiency, operational simplicity, rapid processing, and the production of pure products due to the release of volatile impurities at elevated temperatures. A promising way of igniting combustion synthesis reactions is hybrid microwave heating where the sample is heated both by interaction with microwaves and by heat originating from a microwave-absorbing susceptor in contact with the sample (Rosa et al., 2013).

In this work, *in situ* intermetallic matrix composites are obtained by combustion synthesis triggered by hybrid microwave heating. The main novelty of this work lies in the use of waste alloy powders (Inconel 625, Ti6Al4V and AlSi10Mg) from selective laser melting (SLM) to produce macroalloyed NiAl and TiAl. Waste powder from SLM processing is currently an economic and environmental issue that need to be addressed (Powell et al., 2020) It is hypothesized that the alloying elements in the recycled powders may result in interesting multiphase microstructures and solid solution strengthening of the aluminides. Microstructural investigations by X-ray powder diffraction (XRD) and scanning electron microscopy (SEM) are presented. It will be shown that the combination of low-energy processing and recycled reagents is a viable option to synthesize green materials.

2. Experimental

Exhauste powders of Inconel 625 (Ni source), AlSi10Mg (main Al source) and Ti6Al4V (Ti source) were used as reagents. Target NiAl compositions were obtained by mixing Inconel 625 and AlSi10Mg powders to achieve Ni:Al atomic ratios of 30:70, 40:60, 50:50, 60:40, and 70:30. For the TiAl-based system, AlSi10Mg and Ti6Al4V powders were mixed to achieve Al:Ti atomic ratios of 50:50, 60:40, and 70:30. The final atomic compositions are reported in Table 1. The powder mixtures were prepared by weighting each component in polypropylene container followed by tumbling mixing. Mixed powders (10g) were uniaxial pressed (300 MPa) in a steel mold (∅ 25 mm). The pressed powders were ignited using a rectangular wave guide applicator (86×43 mm cross section) and a solid state microwave generator (2.45 GHz, 200 W). Real-time values of the forward and reflected power given by the generator allowed to perform impedance matching using the three-stub tuner and the shorting plunge. The sample was positioned at the center of the waveguide cavity and supported by a refractory material, on which a silicon carbide disc was placed to serve as a co-absorber.

Table 1. Atomic compositions (%) of the powder mixtures used to produce *in situ* intermetallic matrix composites by reactive sintering.

	30Al70Ni	40Al60Ni	50Al50Ni	60Al40Ni	70Al30Ni	50Al50Ti	60Al40Ti	70Al30Ti
Ni	47.16	41.93	36.29	30.19	23.59	-	-	-
Al	20.21	27.95	36.29	45.29	55.05	46.71	55.62	64.39
Ti	-	-	-	-	-	46.71	37.08	27.60
Cr	19.84	17.64	15.27	12.70	9.92	-	-	-
Si	2.17	3.00	3.89	4.86	5.90	4.42	5.49	6.55
Mo	5.11	4.54	3.93	3.27	2.55	-	-	-
Nb	2.06	1.83	1.58	1.32	1.03	-	-	-
Fe	3.34	2.97	2.57	2.14	1.67	-	-	-
Mg	0.10	0.1	0.18	0.22	0.27	0.20	0.25	0.30
V	-	-	-	-	-	1.95	1.55	1.15

Scanning electron microscopy (SEM) imaging coupled with energy-dispersive X-ray spectroscopy (EDS) for chemical analyses were performed on samples following metallographic preparation using an environmental SEM (ESEM, FEI Quanta 200) equipped with an Oxford INCA-350 EDS system. Phase identification were performed using X-ray diffraction (XRD) data collected from metallografically prepared samples. Data were collected using a third generation Empyrean diffractometer (Malvern-Panalytical). Data were collected in the angular range 10-100° 2θ using a step size of 0.0263°2θ and 2.64s/step. Phase identification was performed using the X'Pert Highscore plus software (version 5.1, Malvern Panalytical).

3. Results and discussions

3.1. NiAl pseudo-binary system

Fig. 1 shows BE-SEM images of the samples in the pseudo-binary systems NiAl. The phases present in the composites were determined by XRD and the results are shown in Table 2. The sample with a Ni:Al atomic ratio of 30:70 is composed of B2 NiAl surrounded by a fcc solid solution in which precipitation of Laves C14 (microalloyed $NbCr_2$, bright area in Fig. 1a) is observed. Cr-rich precipitates are observed in the NiAl grains, likely formed due to the higher solubility of Cr in NiAl at high temperatures that precipitates upon cooling (Han & Nemoto, 1999). The Ni-rich FCC solid solution is observed only in this sample because the Al concentration was too low to fully consume Ni in the formation of aluminide phases. This composite could potentially be a ductile-phase toughened intermetallic matrix composite with precipitation strengthening of both the brittle (B2 NiAl matrix) and ductile (Ni-fcc) phase (Misra et al., 2001). The samples with Ni:Al ratios in the mid-range (40Al60Ni-50Al50Ni)) are composed of B2 NiAl as a main phase surrounded by intermetallic phases including Laves C14 structure ($NbCr_2$) and minor σ-phase (CrFe prototype). The 50Al50Ni sample also includes the A15 phase (Cr_3Si prototype). The samples with the Ni:Al ratio of 60Al40Ni still has B2 NiAl as main phase but weak diffraction reflections of Al_3Ni_2 and Al_3Ni are observed (not shown here). The intergranular region is composed of a fine two-phase structure of B2 NiAl and Cr_3Si-type structure (see Fig. 1d). This type of intermetallic composites of aluminides and silicides has not investigated previously as far as the authors are aware of. Sample 70Al30Ni results in a mixture of Al_3Ni_2 and Al_3Ni in addition to some minor NiAl (weak diffraction reflections, not shown here). The intergranular area is composed Cr_3Si and Cr5Si3. A common feature of the Cr silicides is that they contain variable amounts of the 4d transition metals brought in by the Ni-source (not shown here).

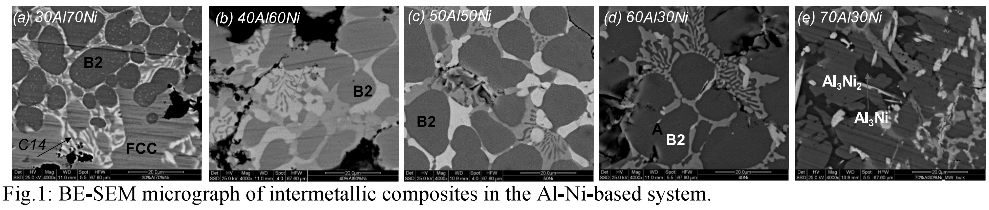

Fig.1: BE-SEM micrograph of intermetallic composites in the Al-Ni-based system.

Table 2. Phases in the Al-Ni-based system (red=absent; green=present).

Phase	Structurbericht/ Pearson symbol	Prototype	Space group	30Al	40Al	50Al	60Al	70Al
Ni-fcc	A1/*cP*2	Cu	*Fm*-3*m*					
NiAl	B2/*CF*4	CsCl	*Pm*-3*m*					
Laves ($NbCr_2$)	C14/*hP*12	$MgZn_2$	*P*63/*mmc*					
σ-phase	$D8_b$/*tP*30	CrFe	*P*42/*mmm*					
Cr_3Si	A15/*cP*8	Cr_3Si	*Pm*-3*m*					
Al_3Ni_2	$D5_{13}$/*hP*5	Al_3Ni_2	*P*-3*m*1					
Al_3Ni	$D0_{22}$/*tI*8	Al_3Ti	*I*4/*mmm*					
Cr_5Si_3	$D8_m$/*tI*32	W_5Si_3	*I*4/*mcm*					

3.2. TiAl pseudo-binary system

Fig. 2 shows backscattered electron (BE) SEM images of the various intermetallic matrix composites in the pseudo-binary systems TiAl (50-70 at. % aluminum) whereas Table 3 shows the phases identified by XRD. Common for all samples is that they are composed of a continuous Ti aluminide matrix containing precipitated elongated Si_5Ti_3 crystals (Fig. 2).

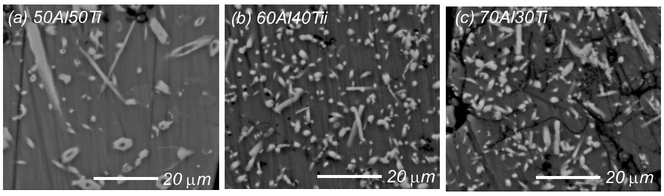

Fig. 2: BE-SEM micrograph of intermetallic composites in the Al-Ti-based system.

Table 3. Phases in the Al-Ti-based system (red=absent; green=present).

Phase	Structurbericht/ Pearson symbol	Prototype	Space group	50Al	60Al	70Al
γ-TiAl	$L1_0$/*tP*4	CuAu	*P*4/*mmm*			
Si_3Ti_5	$D8_8$/*hP*16	Mn_5Si_3	*P*63/*mcm*			
α-Ti	A3/*hP*2	Mg	*P*63/*mmc*			
Al_2Ti		$ZrGa_2$	*Cmmm*			
Al_3Ti	$D0_{22}$/tI8	Al_3Ti	*I*4/*mmm*			

The matrix is composed of γ-TiAl, Al_2Ti and Al_3Ti in samples with 50, 60 and 70 at.% Al, respectively. Minor unreacted α-Ti is observed in the two samples with lowest Al content (see Table 3). No vanadium intermetallics are observed which indicates microalloying of the main phases (Takahashi et al., 1996).

4. Conclusions

Combustion reactions triggered by a microwave-assisted method can be used to produce *in situ* intermetallic matrix composites of Ni and Ti aluminides using recycled powders of Inconel 625, Ti6Al4V and Al10SiMg. While further investigation is required to fully assess the engineering potential of these systems, this study establishes a proof of concept and introduces a promising pathway for upcycling a class of waste materials destined to become more important due to the increasing demand for additively manufactured components. Moreover, the wide range of Ni-Al- and Ti-based alloy powders available in additive manufacturing provides considerable flexibility to tailor chemical compositions and optimize material outcome.

References

Awotunde, M.A., Ayodele, O.O., Adegbenjo, A.O. et al. (2019). NiAl intermetallic composites—a review of processing methods, reinforcements and mechanical properties. International Journal of Advanced Manufacturing Technology 104, 1733–1747 https://doi.org/10.1007/s00170-019-03984-9

Cotton J.D., Noebe R.D., Kaufman M.J. (1993). The effects of chromium on NiAl intermetallic alloys: Part I. microstructures and mechanical properties. Intermetallics 1, 3-20. https://doi.org/10.1016/0966-9795(93)90016-O

Darolia R. (1991). NiAl alloys for high-temperature structural applications. Journal Of Minerals, Metals & Materials Society 43, 44–49. https://doi.org/10.1007/BF03220163

Deevi S.C., Sikk V.K. (1996). Nickel and iron aluminides: an overview on properties, processing, and applications. Intermetallics 4, 315–331. https://doi.org/10.1016/0966-9795(95)00056-9

Diao G., He A., Wu M., Tang Y., Chen W.G., Li Q.Y., Li D (2024). Lightweight Al_3Ti-based medium-entropy alloys with well-balanced strength and ductility. Scripta Materalia 242, 115928 https://doi.org/10.1016/j.scriptamat.2023.115928

Genc O., Unal R. (2022). Development of gamma titanium aluminide (γ-TiAl) alloys: A review. Journal of Alloys and Compounds 929, 167262. https://doi.org/10.1016/j.jallcom.2022.167262

Han C.S., Nemoto M. (1999). Precipitation of α-Cr in B2-ordered NiA. Intermetallics 7, 59-67. https://doi.org/10.1016/S0966-9795(98)00015-6

Misra A., Gibala R., Noebe R.D. (2001). Optimization of toughness and strength in multiphase intermetallics, Intermetallics 9, 971-978. https://doi.org/10.1016/S0966-9795(01)00098-X

Noebe R.D., Bowman R.R., Nathal M.V. (1993). Physical and mechanical properties of the B2 compound NiAl. International Materials Reviews 38, 193-232. https://doi.org/10.1179/imr.1993.38.4.193

Novák P., Michalcová A., Šerák J., Vojtěch D., Fabián T., Randáková S., Průša F., Knotek V., Novák M. (2009). Preparation of Ti–Al–Si alloys by reactive sintering. Journal of Alloys and Compounds 470, 123–126. https://doi.org/10.1016/j.jallcom.2008.02.046

Paul A.R., Dumbre J., Qiu D., Easton M., Mazur M., Mukherjee M. (2024). Grain refinement and morphological control of intermetallic compounds: A comprehensive review. Current Opinion in Solid State and Materials Science 33, 101200. https://doi.org/10.1016/j.cossms.2024.101200

Powell D., Rennie A.E.W., Geekie L., Burns N. (2020). Understanding powder degradation in metal additive manufacturing to allow the upcycling of recycled powders. Journal of Cleaner Production 268, 122077. https://doi.org/10.1016/j.jclepro.2020.122077

Rosa R., Veronesi P., Leonelli C. (2013). A review on combustion synthesis intensification by means of microwave energy. Chemical Engineering and Processing: Process Intensification 71, 2–18. https://doi.org/10.1016/j.cep.2013.02.007

Schuster J.C., Palm M. (2006). Reassessment of the binary Aluminum-Titanium phase diagram. Journal of Phase Equilibria and Diffusion 27, 255–277. https://doi.org/10.1361/154770306X109809

Shao W., Guevara-Vela J.M., Fernández-Caballero A., Liu S., Llorca J. (2023). Accurate prediction of the solid-state region of the Ni–Al phase diagram including configurational and vibrational entropy and magnetic effects. Acta Materialia 253, 118962. https://doi.org/10.1016/j.actamat.2023.118962

Takahashi, T., Iwami, K., Hasegawa, T. (1996). Alloying Effect of Vanadium Upon Structure and Strength of δ-Phase Titanium Trialuminide. MRS Online Proceedings Library 460, 91–96. https://doi.org/10.1557/PROC-460-91

Wang L., Su Y., Yao C., Huang Y., Shen J., Zhang Y., Liu G., Zhao P., Zhang G. (2022). Microstructure and mechanical property of novel NiAl-based hypoeutectic/eutectic/hypereutectic high-entropy alloy. Intermetallics 143, 107476. https://doi.org/10.1016/j.intermet.2022.107476

Xiao H., Baker I. (1994). Long range order and defect concentrations in NiAl and CoAl, Acta Metallurgica et Materialia 42, 1535-1540. https://doi.org/10.1016/0956-7151(94)90363-8

Yamaguchi M., Inui H., Ito K. (2000). High-temperature structural intermetallics. Acta Materialia 48, 307–322. https://doi.org/10.1016/S1359-6454(99)00301-8

Zharov M.V. (2023). Comparative analysis of features of technologies for obtaining quality spherical powder of nickel aluminide NiAl. Metallurgist 66, 1401-1411. https://doi.org/10.1007/s11015-023-01455-x